Supplementary Information:

Evolutionary development of redundant nuclear localization signals in the mRNA export factor NXF1

Zi Chao Zhang[a], Neal Satterly[b], Beatriz M.A. Fontoura[b] and Yuh Min Chook[a]

[a] Department of Pharmacology, [b] Department of Cell Biology, University of Texas Southwestern Medical Center at Dallas, Dallas, TX, USA.

Table S1. Binding affinity of *hs*NXF1-N fragments for Kapβ2

Karyopherin	***hs*NXF1-N fragments**	**K_D[a] (nM)**	**ΔH (kcal/mol)**	**TΔS[b] (kcal/mol/K)**
Kapβ2	1-109	40±13	-17.21±1.25	-7.31±1.42
	30-109	91±13	-18.51±1.13	-9.16±1.12
	1-92	54±4	-19.57±0.05	-9.82±0.03
	1-80	109±33	-17.74±0.89	-8.40±0.88
	30-80	204±29	-19.16±1.31	-10.17±1.40

[a] Stoichiometry = 0.9-1.1.
[b] TΔS= ΔH – ΔG.
All experiments were performed 3-5 times (± standard deviation)

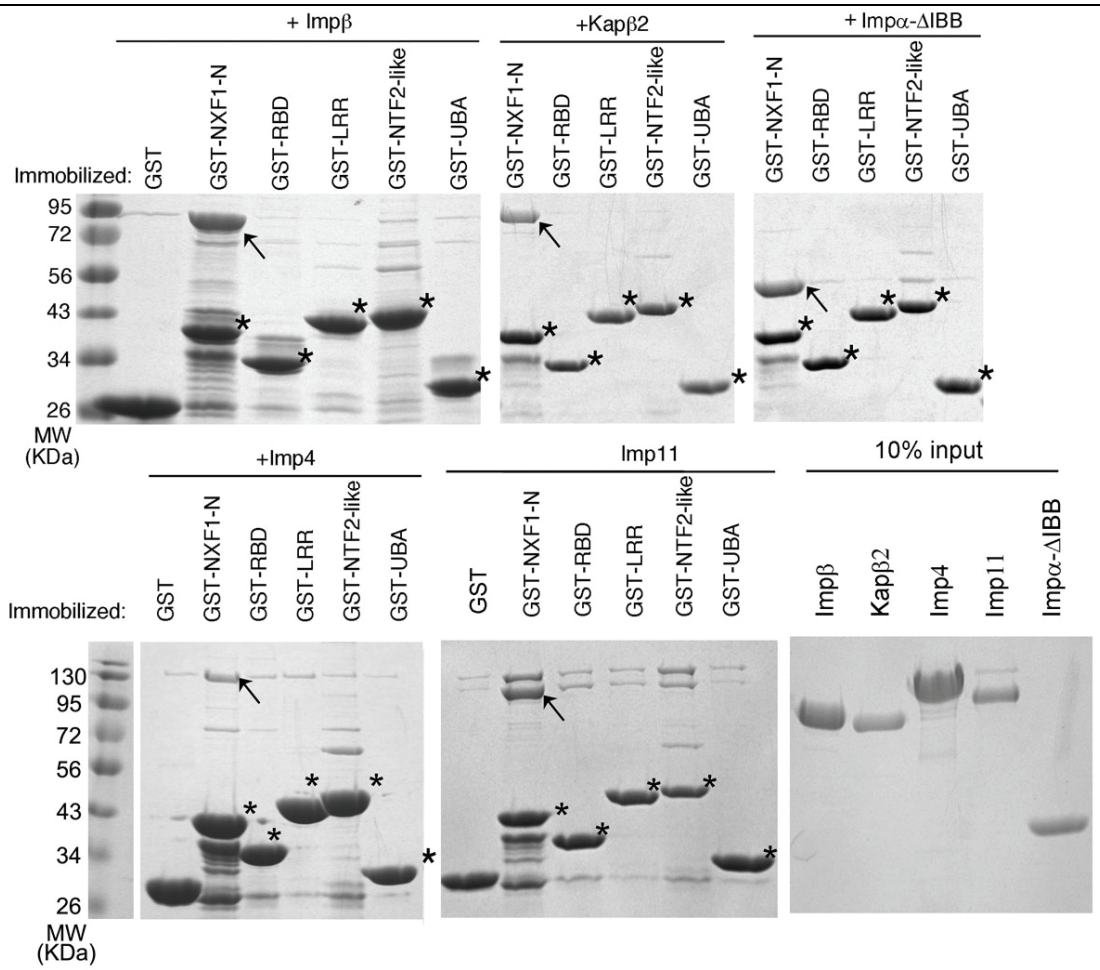

Fig. S1. *hs*NXF1 binds different Karyopherins through its N-terminal tail or *hs*NXF1-N. Individual domains of *hs*NXF1 were expressed as GST fusion proteins, immobilized onto GSH sepharose and then incubated with purified recombinant Karyopherins. Bound proteins and 10% of input Karyopherins were visualized using Coomassie staining. Asterisks, GST-*hs*NXF1 fragments; arrows, Karyopherins.

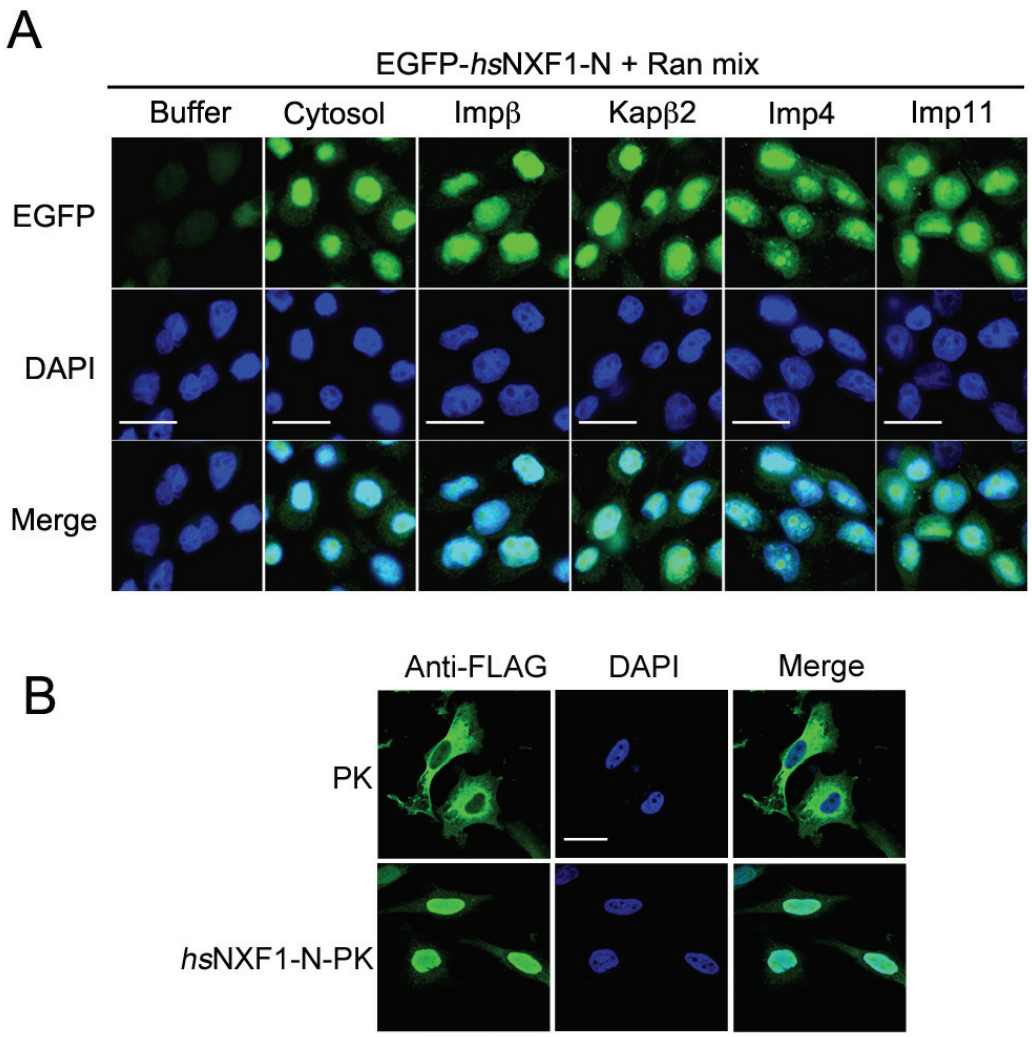

Fig. S2. *hs*NXF1-N is sufficient for nuclear import. *(A)* Nuclear import assays were performed in digitonin-permeabilized HeLa cells with MBP-EGFP-*hs*NXF1-N in the presence of purified Kapβs or buffer. Samples were fixed and stained with DAPI, then subjected to immunofluorescence analysis *(B) hs*NXF1-N was fused to the N-terminus of pyruvate kinase (PK) gene and cloned into pFLAG-CMV vector and transfected into HeLa cells. *hs*NXF1-N-PK was detected by immunofluorescence using anti-Flag antibodies. Scale bar, 10 μm.

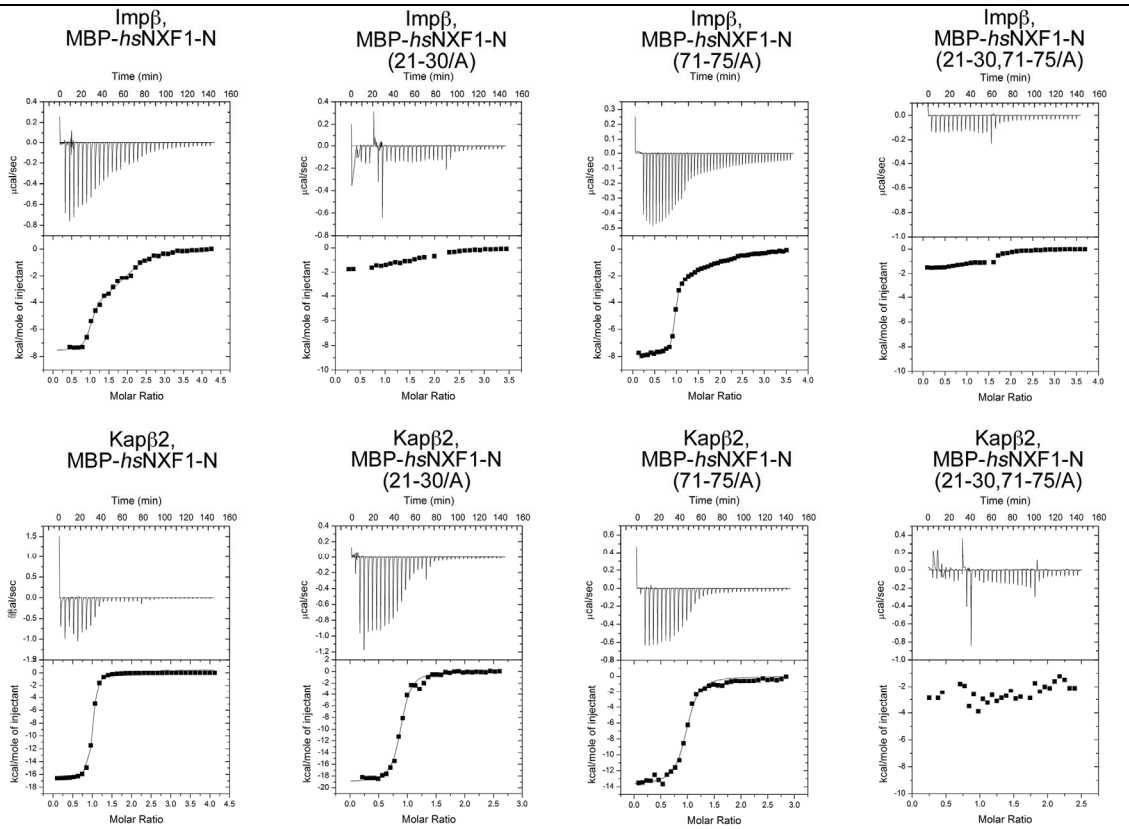

Fig. S3. Selected ITC measurements of MBP-*hs*NXF1-N proteins biniding to Impβ and Kapβ2. After dialyzed against the same buffer, about 100–300 μM MBP-*hs*NXF1-N proteins were titrated into a sample cell containing 10–20 μM recombinant Impβ or Kapβ2 . The experiments were performed at 20°C with either 35 rounds of 8 μl injections or 56 rounds of 6 μl injections. Data were plotted and analyzed using MicroCal Origin software (version 7.0).

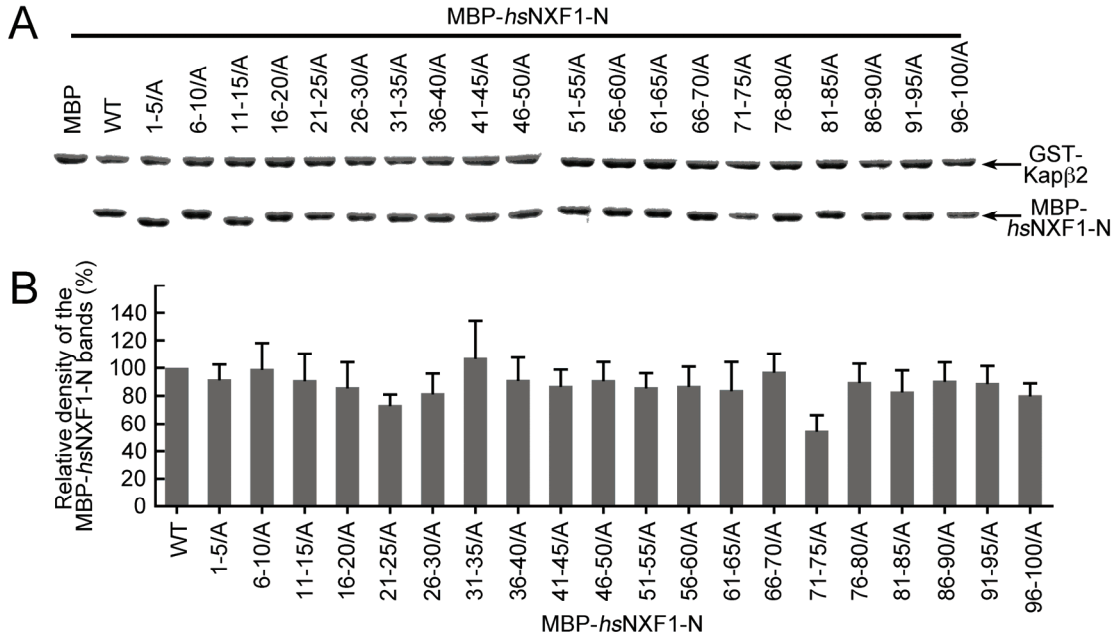

Fig. S4. Mapping *hs*NXF1-N for Kapβ2 binding determinants. *(A)* Every five residues of *hs*NXF1-N (MBP fusion protein) were mutated into alanines and incubated with immobilized GST-Kapβ2. Bound proteins were visualized using Coomassie staining. *(B)* Gels in *(A)* were subjected to densitometry analysis. The density of the MBP-*hs*NXF1-N band in each lane was divided by the density of GST-Kapβ2 in the same lane ($\mathbf{D}_{\text{MBP-}hs\text{NXF1-N}}/\mathbf{D}_{\text{GST-Kap}\beta2}$). The ratios were then normalized to the ratios of MBP-*hs*NXF1-N(WT) *vs.* GST-Kapβ2. Averages of 3 densitometry scans of the gels in *(A)* are shown in the histogram.

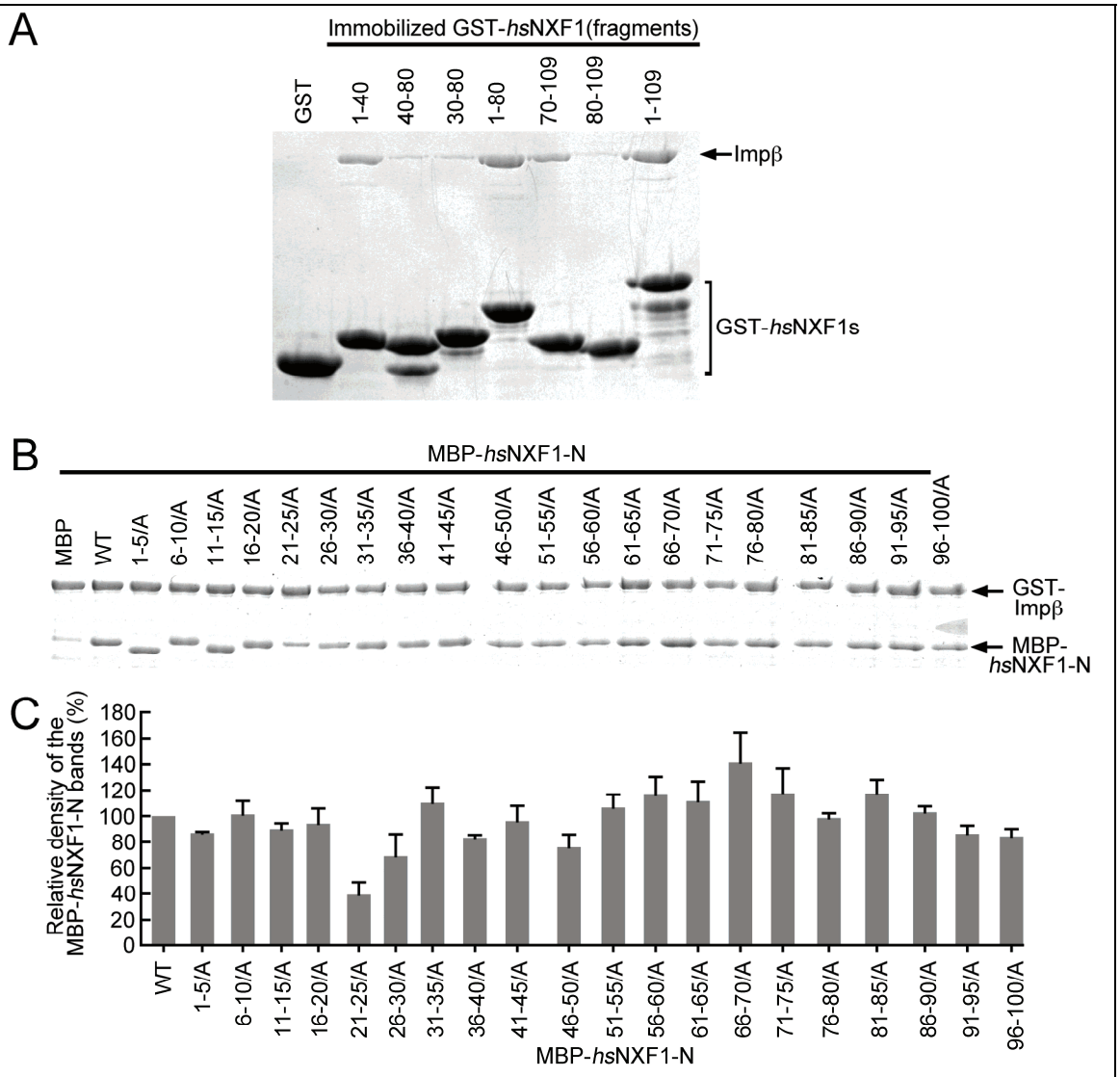

Fig. S5. Mapping *hs*NXF1-N for Impβ binding determinants. *(A)* Immobilized GST fusion proteins of *hs*NXF1-N fragments were incubated with purified recombinant Impβ. *(B)* Every five residues of *hs*NXF1-N (MBP fusion protein) were mutated into alanines and incubated with immobilized GST-Impβ. Bound proteins in *(A)* and *(B)* were visualized using Coomassie staining. *(C)* Gels in *(B)* were subjected to densitometry analysis. The density of the MBP-*hs*NXF1-N band in each lane was divided by the density of GST-Impβ in the same lane ($\mathbf{D}_{\text{MBP-}hs\text{NXF1-N}}/\mathbf{D}_{\text{GST-Imp}\beta}$). The ratios were then normalized to the ratios of MBP-*hs*NXF1-N(WT) *vs.* GST-Impβ. Averages of 3 densitometry scans of the gels in *(B)* are shown in the histogram.

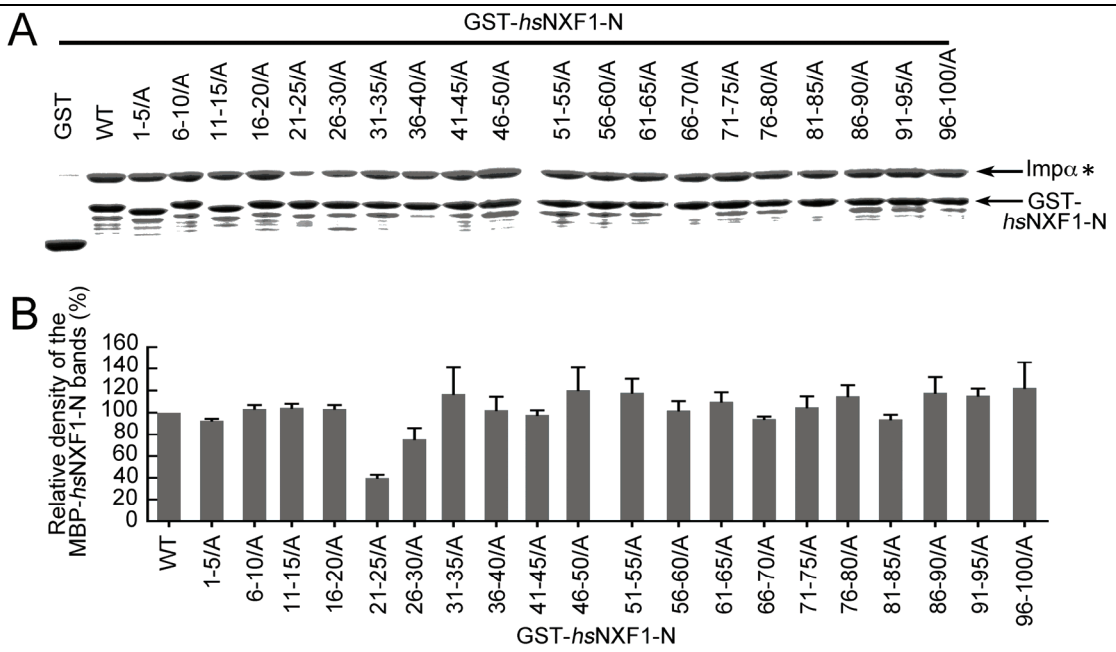

Fig. S6. Mapping *hs*NXF1-N for Impα binding determinants. *(A)* Every five residues of *hs*NXF1-N (GST fusion protein) were mutated into alanines, immobilized and incubated with purified Impα* (the Impα construct used is missing its N-terminal IBB domain). Bound proteins were visualized using Coomassie staining. *(B)* Gels in *(A)* were subjected to densitometry analysis. The density of the GST-*hs*NXF1-N band in each lane was divided by the density of Impα in the same lane ($\mathbf{D}_{\text{MBP-}hs\text{NXF1-N}}/\mathbf{D}_{\text{GST-Imp}\alpha}$). The ratios were then normalized to the ratios of GST-*hs*NXF1-N(WT) *vs.* Impα. Averages of 3 densitometry scans of the gels in *(A)* are shown in the histogram.

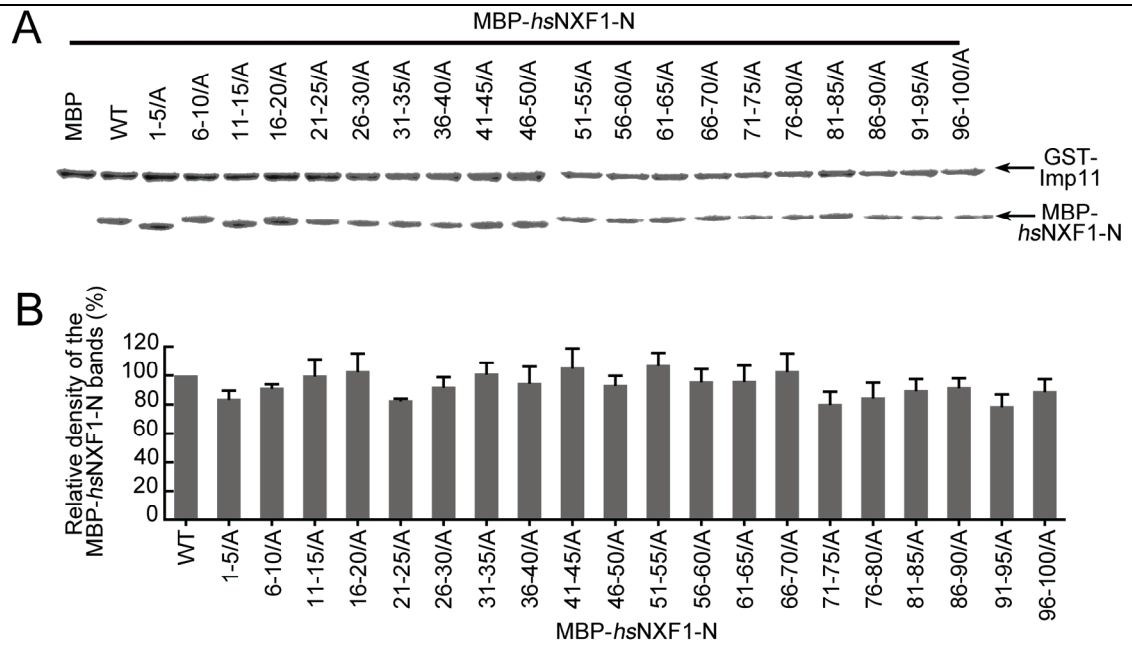

Fig. S7. Mapping *hs*NXF1-N for Imp11 binding determinants. *(A)* Every five residues of *hs*NXF1-N (MBP fusion protein) were mutated into alanines and incubated with immobilized GST-Imp11. Bound proteins were visualized using Coomassie staining. *(B)* Gels in *(A)* were subjected to densitometry analysis. The density of the MBP-*hs*NXF1-N band in each lane was divided by the density of GST-Imp11 in the same lane ($\mathbf{D}_{\text{MBP-}hs\text{NXF1-N}}/\mathbf{D}_{\text{GST-Imp11}}$). The ratios were then normalized to the ratios of MBP-*hs*NXF1-N(WT) *vs.* GST-Imp11. Averages of 3 densitometry scans of the gels in *(A)* are shown in the histogram.

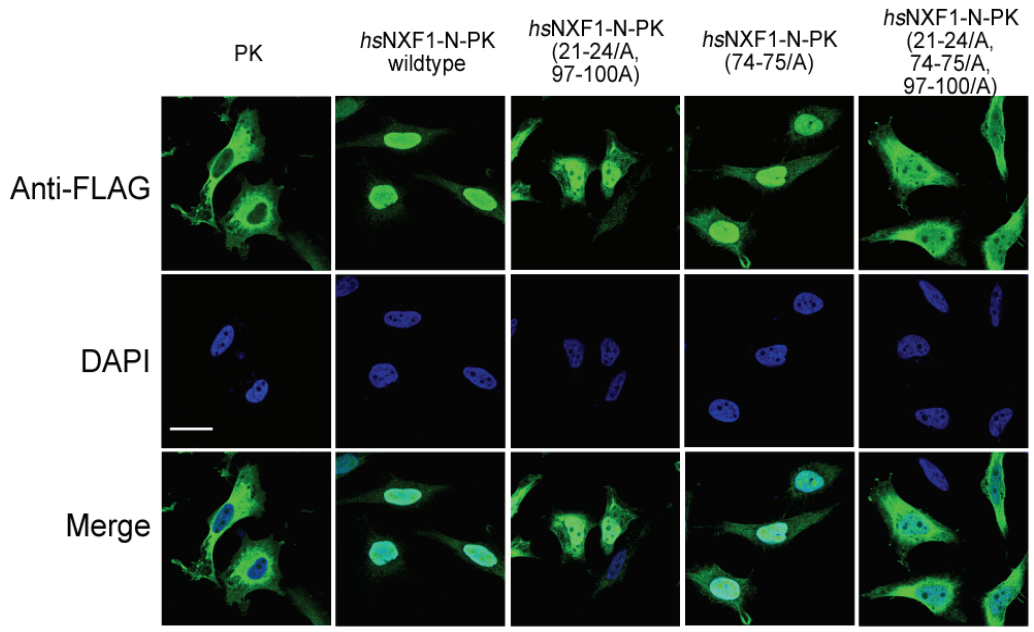

Fig. S8. Mutations in the N-terminal basic NLS epitope and the C-terminal R-$x_{2\text{-}5}$-P-Y NLS epitope diminish nuclear localization of *hs*NXF1-N. Pyruvate kinase (PK) fused to the C-terminus of *hs*NXF1-N proteins were cloned into the pFLAG-CMV2 vector and transfected into HeLa cells. *hs*NXF1-N-PK proteins were detected by immunofluorescence using anti-Flag antibodies. Scale bar, 10 µm.

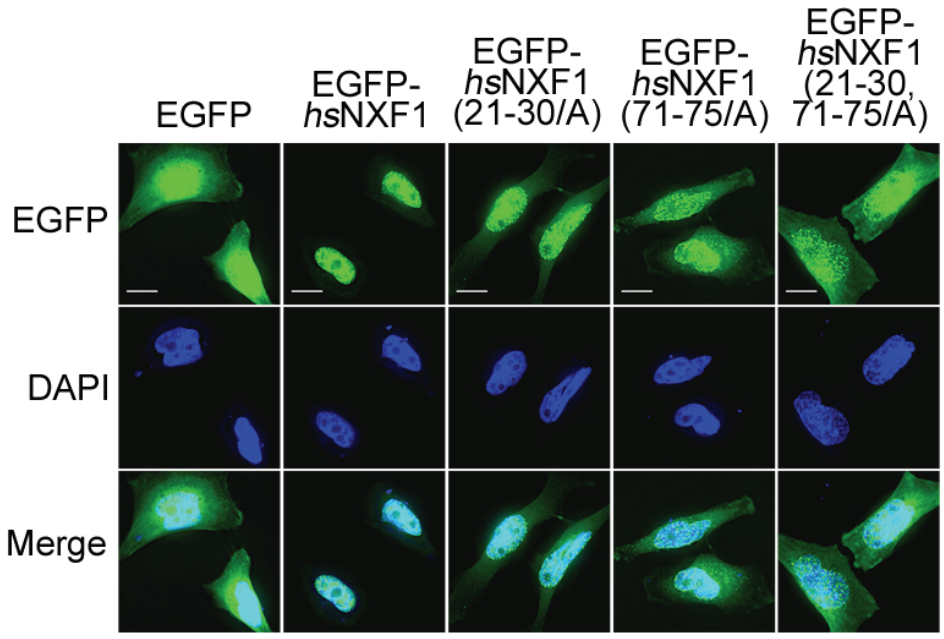

Fig. S9. NLS mutations impair nuclear localization of EGFP-hsNXF1. EGFP-hsNXF1 and its NLS mutants were transfected into HeLa cells. Localization of EGFP fusion proteins were detected by deconvolution microscope. Scale bars, 10μm..

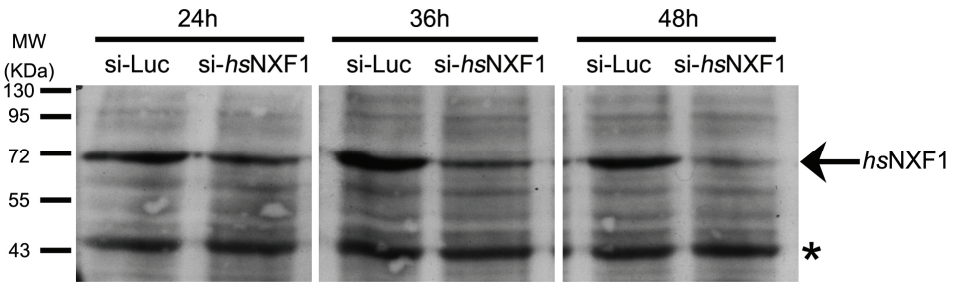

Fig. S10. Knockdown of endogenous *hs*NXF1 by RNAi. Control siRNA targeting Luciferase and siRNA targeting *hs*NXF1 were transfected into HeLa Tet-on cells in 6-well plates using Effectene. Cells were harvested after incubation at 37°C for 24, 36 and 48 hours. The expression levels of endogenous *hs*NXF1 were detected by western blot using mouse anti-NXF1 antibody 53H8 and HRP labeled goat anti-mouse antibody. Asterisk, non-specific bands.

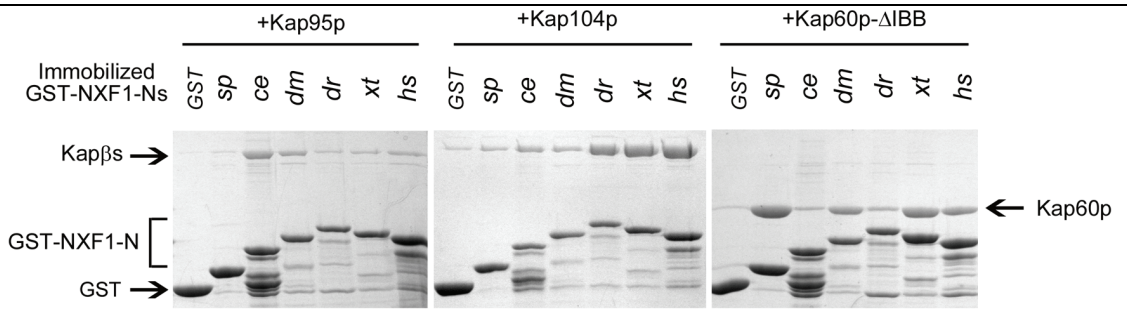

Fig. S11. Interactions of NXF1-Ns from different organisms with S. cerevisiae Kap95p, Kap104p and Kap60p. Immobilized GST-NXF1-Ns of S. pombe, C. elegans, D. melanogaster, D. rerio, X. tropicalis and H. sapiens were incubated with purified recombinant Kap95p, Kap104p and Kap60p-ΔIBB. Bound proteins were visualized using Coomassie staining.